Numerical Characterization of Ultrasound Elastography for the Early Detection of Deep Tissue Injuries

by

Kenton David Hamaluik

Supervisors: Dr. W. Moussa and Dr. M. Ferguson-Pell
Examiner: Dr. R. Burrell
Chair: Dr. M. Zuo

Department of Mechanical Engineering
University of Alberta

June 23, 2014

Contents

Contents

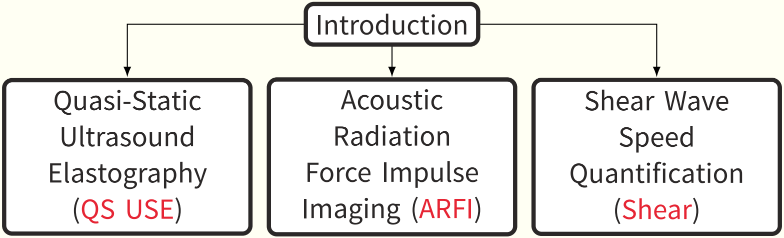
Introduction
Quasi-Static Ultrasound Elastography (QS USE)
Acoustic Radiation Force Impulse Imaging (ARFI)
Shear Wave Speed Quantification (Shear)

Contents

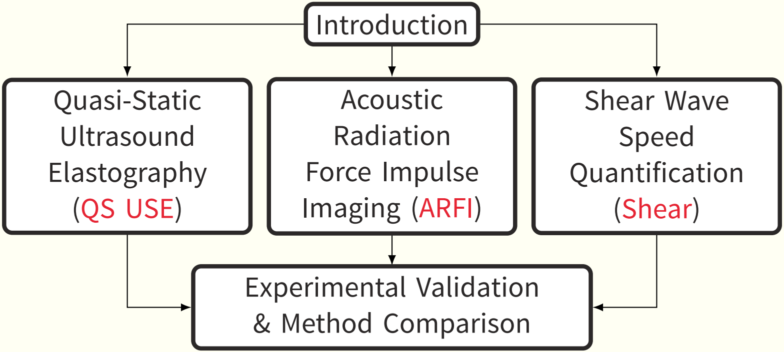
Introduction
Quasi-Static Ultrasound Elastography (QS USE)
Acoustic Radiation Force Impulse Imaging (ARFI)
Shear Wave Speed Quantification (Shear)
Experimental Validation & Method Comparison

Contents

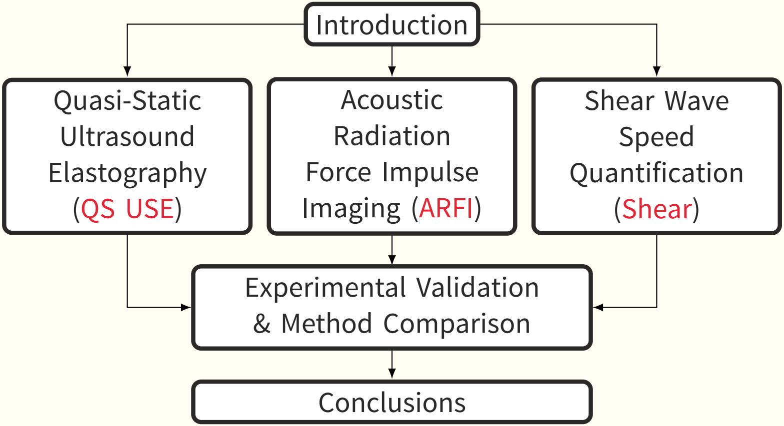
Introduction
Quasi-Static Ultrasound Elastography (QS USE)
Acoustic Radiation Force Impulse Imaging (ARFI)
Shear Wave Speed Quantification (Shear)
Experimental Validation & Method Comparison
Conclusions

Introduction

Deep Tissue Injuries (DTI)

- Secondary injuries (limited mobility)
- Caused by pressure & deformation
- Stage III – IV pressure ulcers
- No clinical detection
- Severe health burdens [Russo et al., 2008]
  - 500,000 – 2,000,000 annually (USA)
  - Increased length of stay, mortality

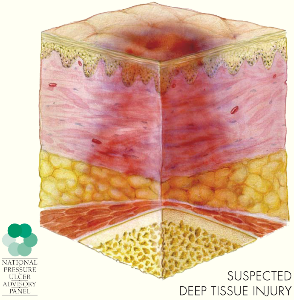

Deep Tissue Injuries (DTI)

- Secondary injuries (limited mobility)
- Caused by pressure & deformation
- Stage III – IV pressure ulcers
- No clinical detection
- Severe health burdens [Russo et al., 2008]
  - 500,000 – 2,000,000 annually (USA)
  - Increased length of stay, mortality

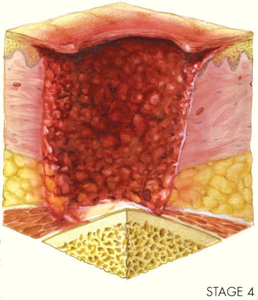

Current DTI Detection

- Clinical settings: risk assessment scales
  - Norton, Braden, and Risk Assessment Pressure Sore scales
  - No actual detection, only risk assessment
- Research settings: MRI
  - Not clinically feasible
- New research:
  - B-mode imaging [Aoi et al., 2009]
  - Blood / urine markers [Makhsous et al., 2010]
  - Ultrasound elastography [Deprez et al., 2011]

Ultrasound Elastography

- Ultrasound elastography is a technology which measures tissue stiffness

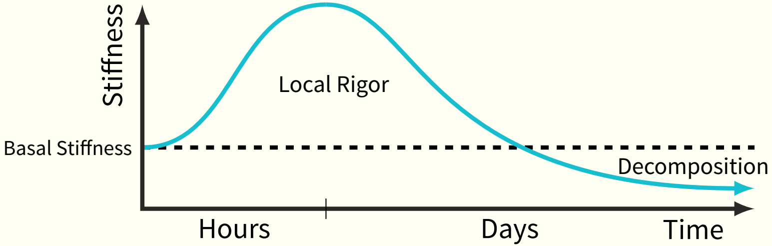

Adapted from [Gefen, 2009], used with permission

- Mechanical stiffness changes with injury formation and progression

Literature Review

- The purpose of this research was understand ultrasound elastography for DTI detection

	DTI	B-Mode US	QS USE	ARFI	Shear	FE Models	Gel Phantoms	Animals	Humans	Characterized	Clinical
PU Risk scales	✗	—	—	—	—	✗	✗	✗	✓	✓	✓
MRI	✓	—	—	—	—	✓	✓	✓	✓	✗	✗
Aoi, 2009	✓	✓	✗	✗	✗	✗	✗	✗	✓	✗	?
Makhsous, 2010	✓	—	—	—	—	—	—	✓	?	✗	✓
Deprez, 2011	✓	✗	✓	✗	✗	✓	✓	✓	?	✗	✓
→ This work	✓	✗	✓	✓	✓	✓	✓	?	?	✓	✓

Quasi-Static Ultrasound Elastography*

* Accepted for publication as: K. Hamaluik, W. Moussa, and M. Ferguson-Pell, “Numerical Characterization of Quasi-Static Ultrasound Elastography for the Detection of Deep Tissue Injuries.” *IEEE Transactions on Medical Imaging*, vol. 33, no. 7, pp. 1410–1421, July 2014.

Theory of Operation

- Manual deformation
- Magnitude of deformation related to stiffness
  - $\downarrow$ deformation

    $\approx \uparrow$ stiffness

    $\approx \uparrow$ damage magnitude

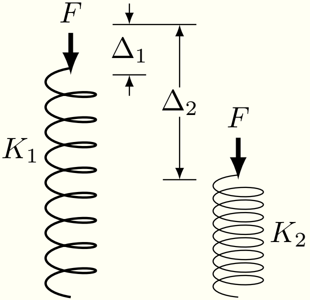

$$\Delta_1 < \Delta_2$$
$$\therefore\ K_1 > K_2$$

Theory of Operation

- Manual deformation
- Magnitude of deformation related to stiffness
  - $\downarrow$ deformation
    $\approx \uparrow$ stiffness
    $\approx \uparrow$ damage magnitude
- Track scattering centres
  - Assumptions of motion [Brusseau et al., 2008]

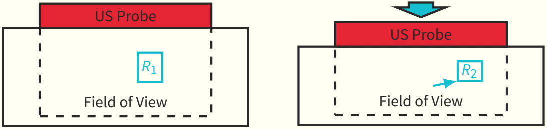

Pre-compression image

Post-compression image

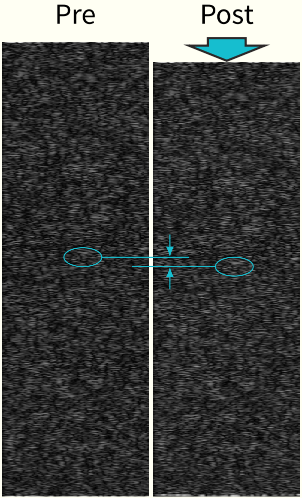

Investigated Models

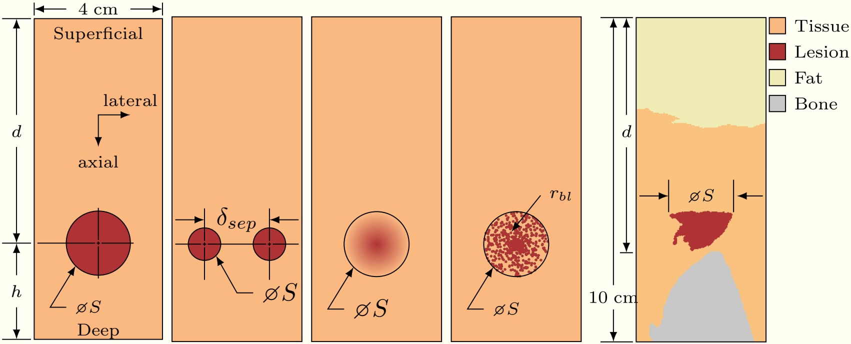

d:	lesion depth	δ_{sep}:	separation distance
h:	lesion altitude	b_r:	blur radius
$\varnothing S$:	lesion size	b_ρ :	cluster density
f:	interrogation frequency	r_{bl}:	cluster radii
ε_{app}:	applied strain		

Sample Simulated Elastogram

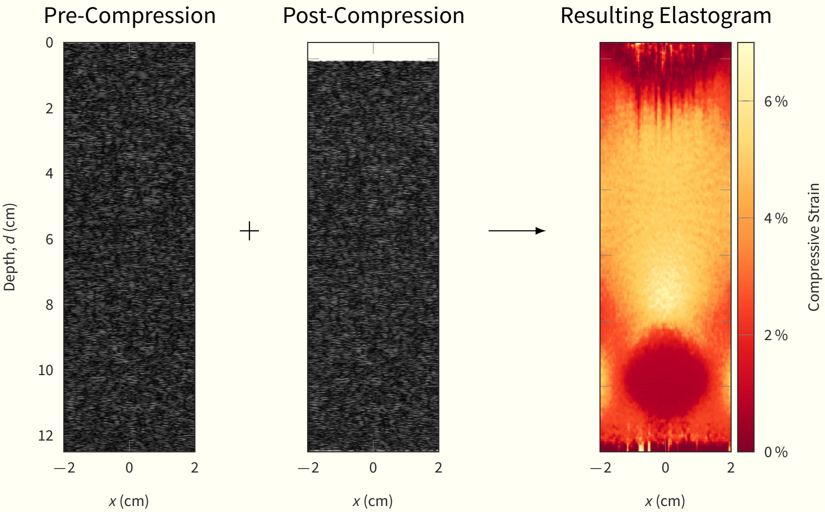

Sample Quasi-Static Results

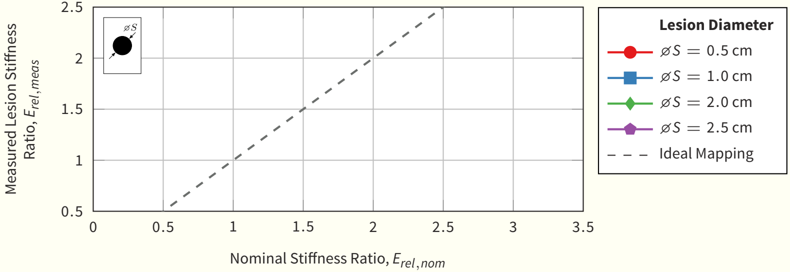

Sample Quasi-Static Results

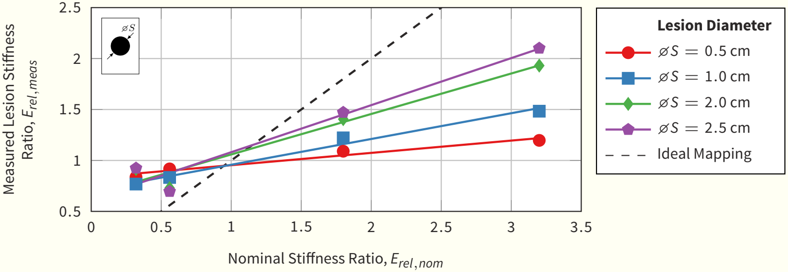

Sample Quasi-Static Results

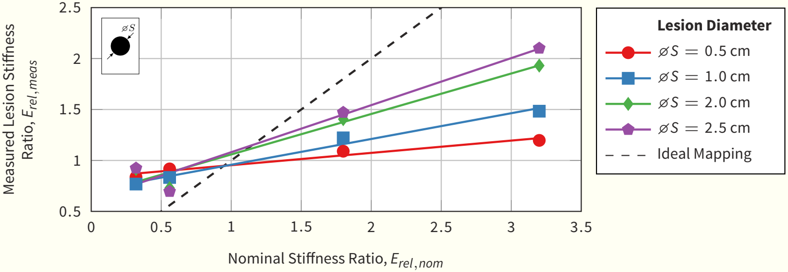

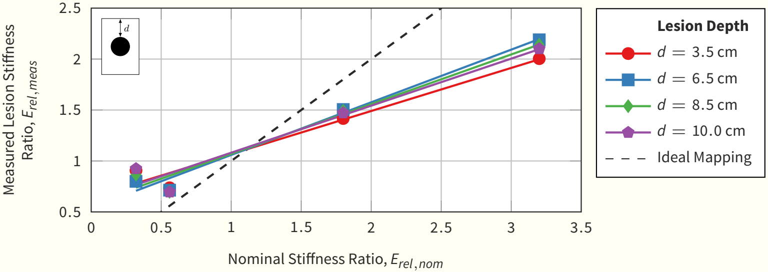

Sample Quasi-Static Results

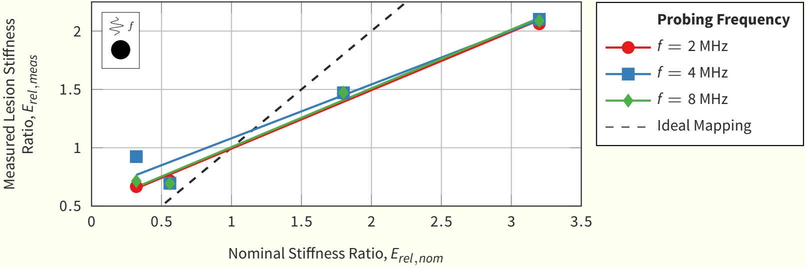

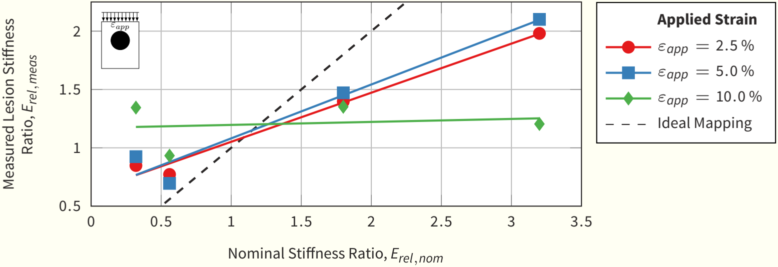

Quasi-Static USE Outcomes

- Small lesions undetectable
  - Larger $\rightarrow$ more accurate
- Not reliant on:
  - Depth
  - Interrogation frequency
- Apply $\lesssim 5\,\%$ strain
- Complicated geometry can affect results
- Not ideally sensitive
- Can detect DTI
- Manual palpation not reliable
  - ARFI imaging as an alternative

Acoustic Radiation Force Impulse Imaging

Introduction

- QS USE has low detection sensitivity, unreliable
- Acoustic Radiation Force Impulse (ARFI) imaging similar to QS USE
  - Transducer-generated force instead of manual
- $\uparrow$ repeatability, $\uparrow$ inter-operator reliability
- Absorbed energy generates force:

$$\left|\vec{F}\right| = \frac{2\alpha I}{c}$$

$\vec{F}$:	ARFI force
α:	Absorption coefficient
I:	Intensity
c:	Longitudinal wave speed

How ARFI Imaging Works

- Normal ultrasound is only a couple periods long (≈ 2 ms)
- ARFI imaging uses continuous beams (≈ 100 ms)

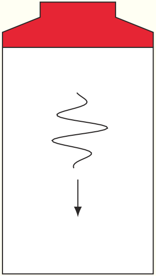

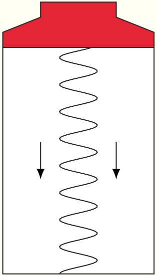

- Absorbed acoustic energy has safety implications

Simulating ARFI Loads

- Use k-space pseudo-spectral method to solve the wave equation
  - k-Wave MATLAB® toolbox

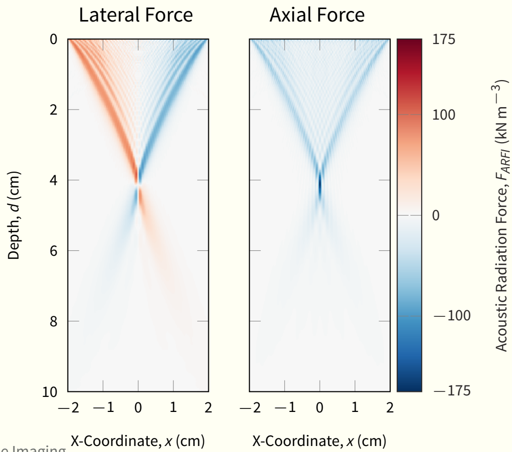

Sample ARFI Results

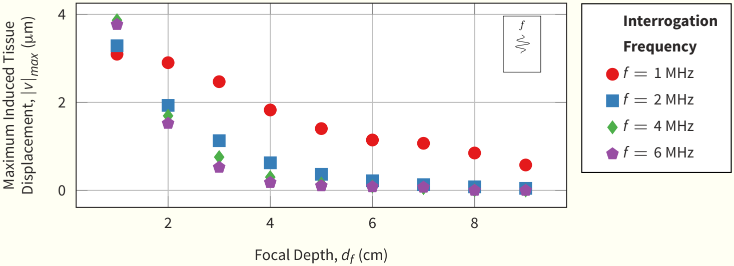

Sample ARFI Results

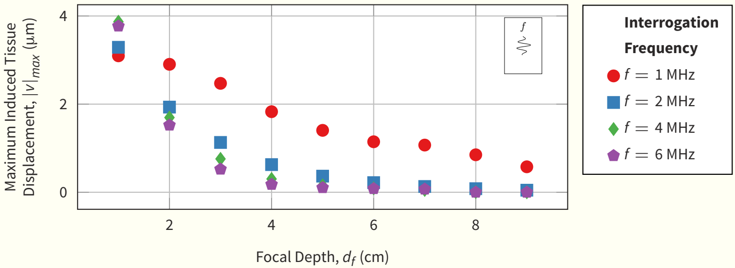

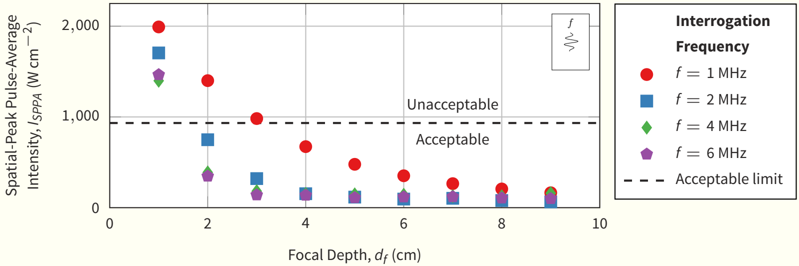

Sample ARFI Results

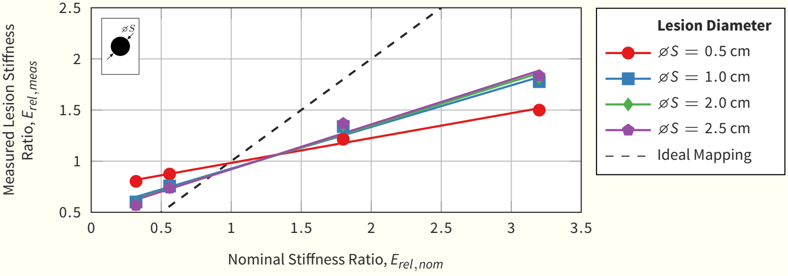

Sample ARFI Results

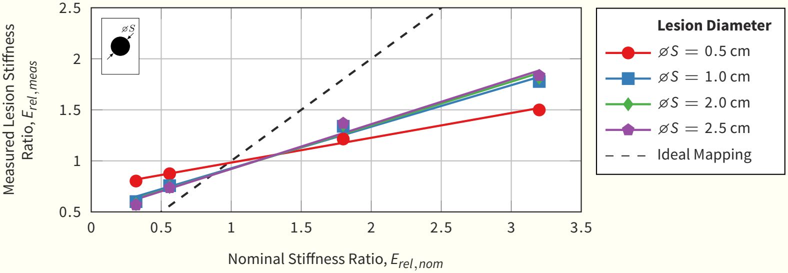

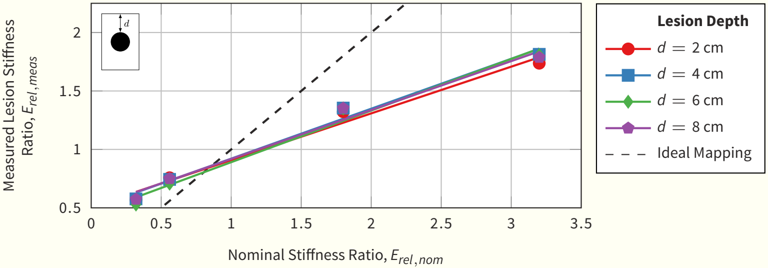

ARFI Imaging Outcomes

- ARFI sensitivity $\approx$ QS USE sensitivity
- ARFI not as dependent on lesion size as QS USE
  - Similar characterization results as QS USE
- Complicated geometry can affect results
- ARFI more reliable than QS USE
- ARFI has limited penetration depth
  - Significant safety considerations

Shear Wave Speed Quantification

Introduction

- QS USE and ARFI provide qualitative measures
- Shear wave speed quantification is quantitative
  - Absolute values
  - Track over time
- Uses ARFI pulses to generate shear waves
  - Measure shear wave speed $\rightarrow$ calculate stiffness:

$$\mu = c_T^2 \rho$$

μ: Shear modulus
c_T: Shear wave speed
ρ: Tissue density

Measuring Shear Wave Speed

1. Induce ARFI at desired depth
   - Shear waves radiate outward, like “ripples in a pond”

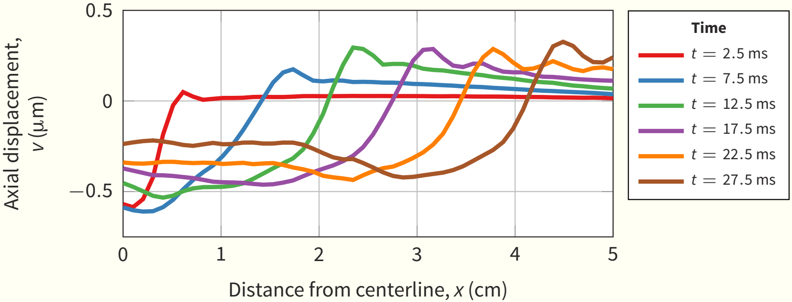

Measuring Shear Wave Speed

1. Induce ARFI at desired depth
   - Shear waves radiate outward, like “ripples in a pond”
2. Monitor deformation along a line extending from the focal point using B-mode ultrasound

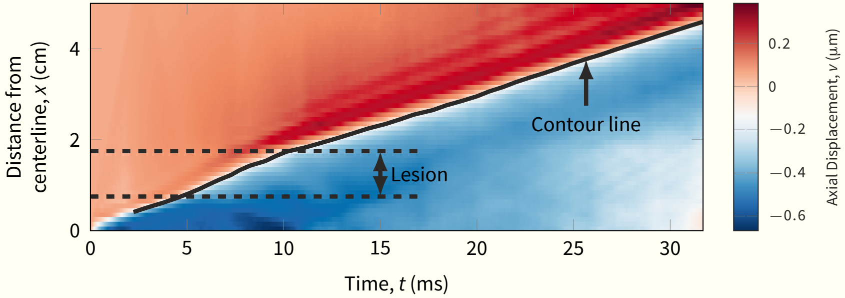

Measuring Shear Wave Speed

1. Induce ARFI at desired depth
   - Shear waves radiate outward, like “ripples in a pond”
2. Monitor deformation along a line extending from the focal point using B-mode ultrasound
   - Calculate speed of shear wave along this line

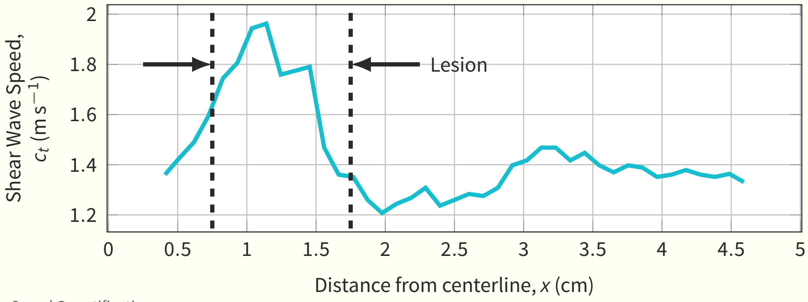

Sample Shear Results

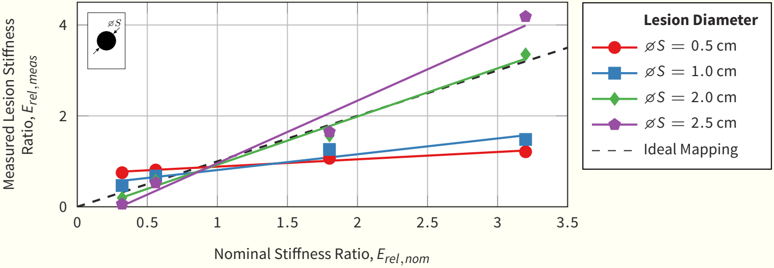

Sample Shear Results

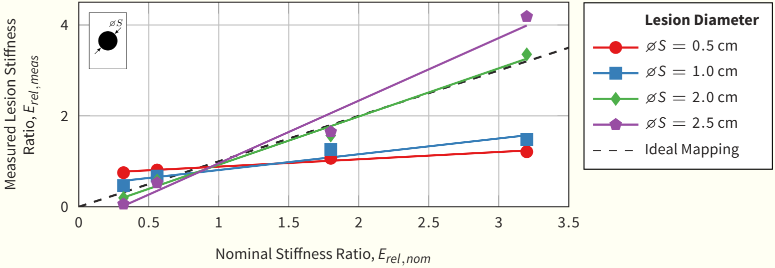

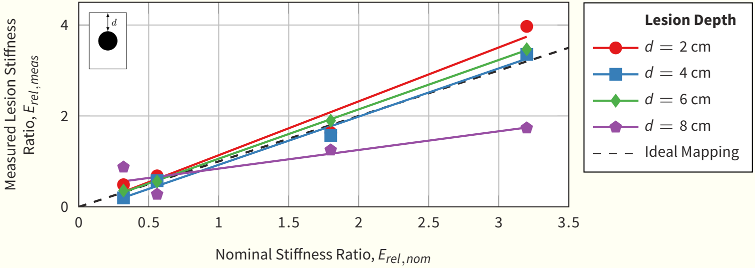

Shear Wave Speed Outcomes

- Similar reliability to ARFI
- Difficult to detect:
  - Small lesions
  - Deep lesions
- Localized measures only
  - QS USE and ARFI provide domain interrogation
- More sensitive than ARFI and QS USE
- Quantifiable
  - Can monitor injury over time

Experimental Validation & Method Comparisons

Experimental Setup

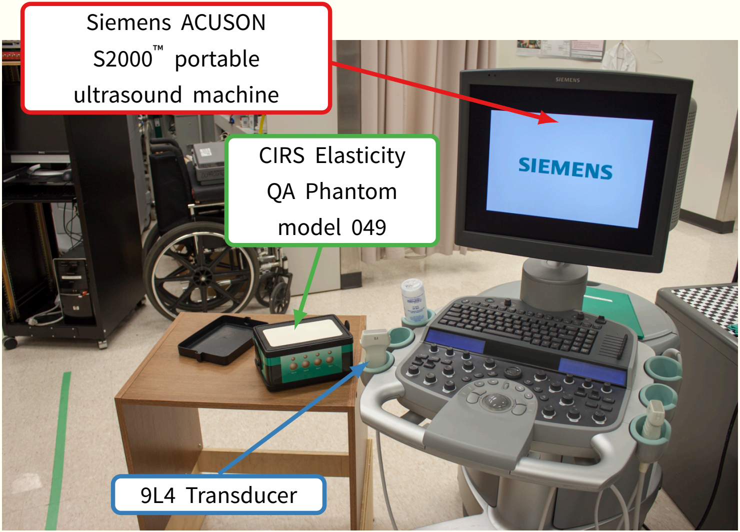

Experimental Validations

- Siemens ACUSON S2000™ ultrasound machine with a Siemens 9L4 transducer and a CIRS QA Phantom 049 gel phantom
- Compared parametrically-identical experimental results to simulation

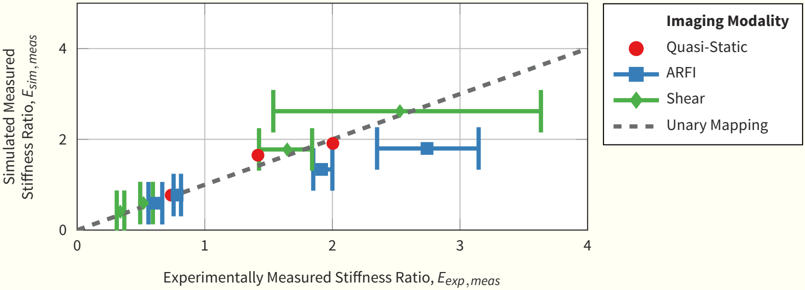

Comparing Methods

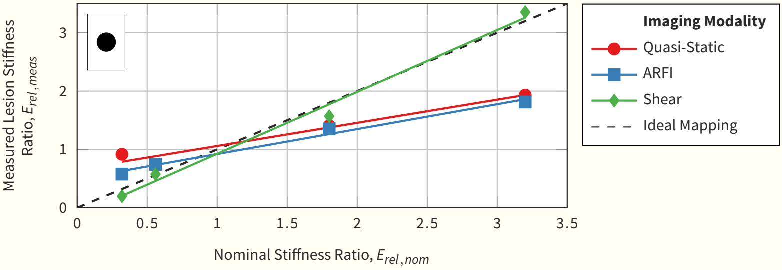

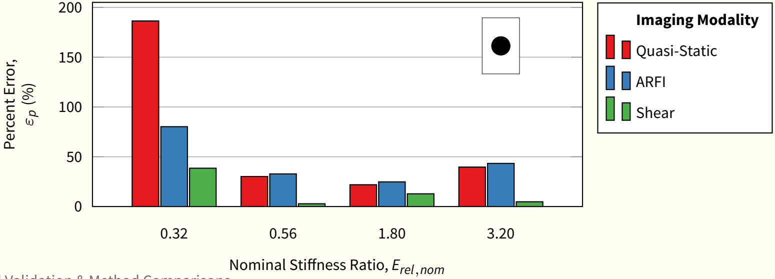

Conclusions

Conclusions

- DTI are a major health concern
  - No early detection
- Ultrasound elastography can detect DTI
  - Within limits
  - Clinically feasible
- Numerically characterized 3 modalities
  - Quasi-Static Ultrasound Elastography
  - Acoustic Radiation Force Impulse Imaging
  - Shear Wave Speed Quantification

Recommendations

- Shear wave speed quantification yields best results
  - Use when possible
- ARFI more reliable than QS USE
  - Lacks penetration depth
- Small lesions ($r \lesssim 0.5\,\text{cm}$) difficult to detect
  - MRI'd lesions: $r \gtrsim 1.0\,\text{cm}$
- Future work: animal and human studies
  - Toward eventual clinical implementation

Thank You

- Supervisors:
  - Dr. W. Moussa
  - Dr. M. Ferguson-Pell
- Lab-mates

Project SMART
Sensory Motor Adaptive Rehabilitation Technology

Additional Slides

- Additional Figures
- References
- Derivation of ARFI
- K-Space Equations
- Quasi-Static Parameters
- ARFI Parameters
- Shear Parameters
- Phantom Properties
- Quasi-Static Finite-Element Details
- Quasi-Static Mesh Dependency
- ARFI / Shear Finite-Element Details
- ARFI / Shear Mesh Dependency

References

[Aoi et al., 2009] Aoi, N., Yoshimura, K., Kadono, T., Nakagami, G., Iizuka, S., Higashino, T., Araki, J., Koshima, I., and Sanada, H. (2009).
Ultrasound assessment of deep tissue injury in pressure ulcers: possible prediction of pressure ulcer progression.
Plastic and reconstructive surgery, 124(2):540–550.

[Brusseau et al., 2008] Brusseau, E., Kybic, J., Deprez, J.-F. F., and Basset, O. (2008).
2-D locally regularized tissue strain estimation from radio-frequency ultrasound images: theoretical developments and results on experimental data.
IEEE transactions on medical imaging, 27(2):145–160.

[Deprez et al., 2011] Deprez, J.-F. F., Brusseau, E., Fromageau, J., Cloutier, G., and Basset, O. (2011).
On the potential of ultrasound elastography for pressure ulcer early detection.
Medical physics, 38(4):1943–1950.

[Gefen, 2009] Gefen, A. (2009).
Deep tissue injury from a bioengineering point of view.
Ostomy/wound management, 55(4):26–36.

[Makhsous et al., 2010] Makhsous, M., Lin, F., Pandya, A., Pandya, M. S., and Chadwick, C. C. (2010).
Elevation in the serum and urine concentration of injury-related molecules after the formation of deep tissue injury in a rat spinal cord injury pressure ulcer model.
PM & R : the journal of injury, function, and rehabilitation, 2(11):1063–1065.

[Russo et al., 2008] Russo, C., Steiner, C., and Spector, W. (2008).
Hospitalizations related to pressure ulcers among adults 18 years and older, 2006: Statistical brief no. 64.
Agency for Health Care Policy and Research (US).

Derivation of Acoustic Force

$$\sigma_{ij,j} + \rho b_i = \rho f_i$$

$$\vec{F} = \nabla p_2 - \mu_{tissue} \nabla^2 \vec{v_2}$$

$$\vec{F} = \rho \langle \vec{v_1} \nabla \cdot \vec{v_1} + \vec{v_1} \nabla \vec{v_1} \rangle$$

$$\vec{F} = 2\rho \langle \vec{v} \vec{v}_{,x} \rangle$$

$$\vec{v} = i\omega A e^{-\alpha x + i(\omega t - kx)} \hat{x}$$

$$\left| \vec{F} \right| = A^2 e^{-2\alpha x} \rho \alpha$$

$$\boxed{\left| \vec{F} \right| = \frac{2\alpha I}{c}}$$

$\langle\rangle$:	Time-average
$\vec{F}$:	Acoustic Force
$\vec{v}$:	Particle velocity
ρ:	Tissue density
α:	Absorption coefficient
I:	Acoustic intensity
c:	Speed of sound

K-Space Equations

$$\nabla^2 P - \frac{1}{c_0^2}\frac{\partial^2 P}{\partial t^2} = 0$$

Momentum conservation, mass conservation, and pressure-density relation in a homogeneous lossless medium:

$$\frac{\partial \vec{v}}{\partial t} = -\frac{1}{\rho_0}\nabla P$$
$$\frac{\partial \rho}{\partial t} = -\rho_0 \nabla \cdot \vec{v}$$
$$P = c_0^2 \rho$$

Momentum conservation, mass conservation, and pressure-density relation in a non-linear heterogeneous lossy medium:

$$\frac{\partial \vec{v}}{\partial t} = -\frac{1}{\rho_0}\nabla P$$
$$\frac{\partial \rho}{\partial t} = -\left(2\rho + \rho_0\right) \nabla \cdot \vec{v} - \vec{v} \cdot \nabla \rho_0$$
$$P = c_0^2 \left(\rho + \vec{u} \cdot \nabla \rho_0 + \frac{B}{2A}\frac{\rho^2}{\rho_0} - \mathbf{L}\rho \right)$$

$$\mathbf{L} = \tau \left(-\nabla^2\right)^{\frac{y}{2}-1} + \eta \left(-\nabla^2\right)^{\frac{y+1}{2}-1}$$

$$\tau = -2\alpha_0 c_0^{y-1}\frac{\partial}{\partial t}\,, \qquad \eta = 2\alpha_0 c_0^{y} \tan\left(\frac{\pi y}{2}\right)$$

QS USE Parameters

QS USE Parametric Study Parameters

Parameter	Symbol	Values	Units
Lesion depth	d	3.5, 6.5, 8.5 and 10.0	cm
Lesion altitude	h	1.25, 2.50 and 3.75	cm
Lesion diameter	$\varnothing S$	0.5, 1.0, 2.0 and 2.5	cm
Lesion stiffness ratio	E_{rel}	0.32, 0.56, 1.80 and 3.20	–
Ultrasound frequency	f	2, 4 and 8	MHz
Transducer-applied strain	ε_{app}	2.5, 5.0 and 10.0	%
Co-located separation distance	δ_{sep}	1.25, 1.50, 1.75 and 2.00	cm
Blurred lesion blur radius	b_r	1.0, 2.5, 5.0 and 7.5	mm
Clustered lesion density	b_ρ	10, 20, 30 and 40	cm^{-2}
Clustered lesion radius	r_{bl}	0.5, 1.0 and 1.5	mm
Visible human lesion width	$\varnothing L$	0.5, 1.0, 2.0 and 2.5	cm
Visible human lesion depth	d	6.25, 6.75 and 7.25	cm

Quasi-Static Default Parameters

Property	Value	Units
Domain Width	4	cm
Domain Depth	12.5	cm
B-Mode Sampling Frequency	50	MHz
B-Mode Probing Frequency	4	MHz
Wave Speed	1540	$m\,s^{-1}$
Basal Stiffness	25	kPa
Tissue Density	1060	$kg\,m^{-3}$
Applied Strain	5	%

ARFI Parameters

K-Space Psuedospectral Model Parameters

Property	Symbol	Value	Units
Nonlinearity parameter	B/A	8	–
Power law prefactor	α_0	0.7	$\mathrm{Np}\,(\mathrm{rad/s})^{-y}\,\mathrm{m}^{-1}$
Power law exponent	y	0.95	–
Density	ρ_0	1060	$\mathrm{kg}\,\mathrm{m}^{-3}$

ARFI Parameters

Simulated Material Parameters

Property	Symbol	Value	Units
Bulk Modulus	K	515.7	kPa
Shear Modulus	μ_{tissue}	1.0	kPa
Density	ρ	1060	$\mathrm{kg\,m^{-3}}$

Generalized Maxwell Viscoelastic Material Model Parameters

Branch	Shear Modulus (Pa)	Relaxation Time (s)
1	791.0	2
2	66.5	40
3	0.6	80

ARFI Parameters

ARFI Parametric Study Parameters

Parameter	Symbol	Values	Units
ARFI interrogation frequency	f	1, 2, 4 and 6	MHz
Transducer width	w_{trans}	4, 8 and 10	cm
ARFI pulse cycles	n_c	3, 100, 300, 500 and 700	–
ARFI source pressure	P_{source}	4, 5, 6, 7 and 8	MPa
Lesion depth	d	1, 2, 3, 4, 5, 6, 7, 8 and 9	cm
Lesion diameter	$\varnothing S$	0.5, 1.0, 2.0 and 2.5	cm
Lesion stiffness ratio	E_{rel}	0.32, 0.56, 1.80 and 3.20	–
Blurred lesion blur radius	b_r	1.0, 2.5, 5.0 and 7.5	mm
Clustered lesion density	b_ρ	10, 20, 30 and 40	cm^{-2}
Clustered lesion radius	r_{bl}	0.5, 1.0 and 1.5	mm
Visible human lesion width	$\varnothing L$	0.5, 1.0, 2.0 and 2.5	cm

ARFI / Shear Default Parameters

Property	Value	Units
Domain Width	4	cm
Domain Depth	10	cm
Acoustic Pressure	3.35	MPa
Probing Frequency	6	MHz
Pulse Cycles	300	–
Sound Speed	1540	$\mathrm{m\,s^{-1}}$
Attenuation Coefficient	0.57	dB/MHzcm
Tissue Density	1060	$\mathrm{kg\,m^{-3}}$
Power law prefactor	0.7	$\mathrm{Np\,(rad/s)^{-y}\,m^{-1}}$
Power law exponent	0.95	–
B/A	8	–
FEA Time-Step	25	ns

Shear Parameters

Shear Parametric Study Parameters

Parameter	Symbol	Values	Units
Lesion depth	d	1, 2, 3, 4, 5, 6, 7, 8 and 9	cm
Lesion diameter	$\varnothing S$	0.5, 1.0, 2.0 and 2.5	cm
Lesion offset	d_{off}	0.00, 1.25, 2.50 and 3.75	cm
Lesion stiffness ratio	E_{rel}	0.32, 0.56, 1.80 and 3.20	
Blurred lesion blur radius	b_r	1.0, 2.5, 5.0 and 7.5	mm
Clustered lesion density	b_ρ	10, 20, 30 and 40	cm^{-2}
Clustered lesion radius	r_{bl}	0.5, 1.0 and 1.5	mm
Visible human lesion width	$\varnothing L$	0.5, 1.0, 2.0 and 2.5	cm

CIRS Phantom Properties

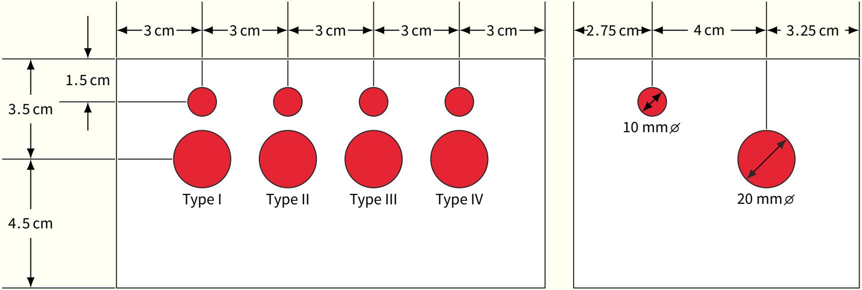

CIRS Phantom Material Properties and Geometry

Property	Symbol	Value	Units
Nominal basal elastic modulus	E_{tissue}	25	kPa
Lesion elastic modulii	E_{tissue}		
Type I		4	kPa
Type II		14	kPa
Type III		45	kPa
Type IV		80	kPa
Speed of sound	c_0	1540	$\mathrm{m\,s^{-1}}$
Acoustic attenuation	α	0.5	$\mathrm{dB\,cm^{-1}\,MHz^{-1}}$

Quasi-Static FEA Details

- Quadratic Lagrangian triangular elements
- 9,468 degrees of freedom
- Solved using COMSOL Multiphysics

$$-\nabla \cdot \sigma = \vec{F}$$

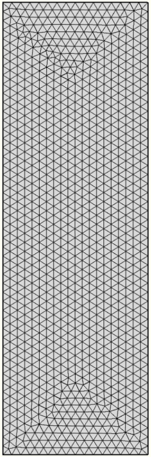

The Quasi-Static Mesh

Quasi-Static Mesh Dependency

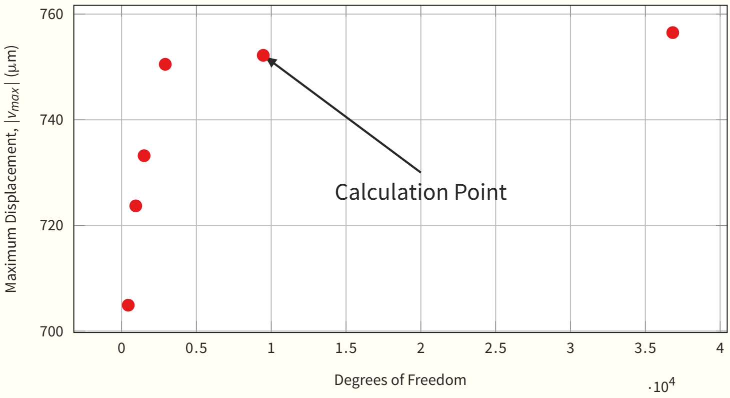

ARFI / Shear FEA Details

- Quadratic Lagrangian triangular elements
- 51,096 degrees of freedom
- 25 ns constant time stepping
- Simulation stopped after focal displacement reached 1 % of maximal value
- Solved using COMSOL Multiphysics

$$\rho \frac{\partial^2 \vec{u}}{\partial t^2} - \nabla \cdot \sigma = \vec{F}$$

$$\sigma - \sigma_0 = C : \varepsilon + \sum_m 2G_m \tau_m \dot{\gamma}_m$$

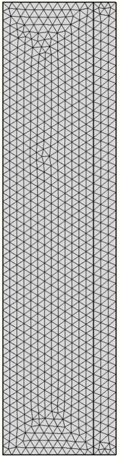

The ARFI / Shear Mesh

ARFI / Shear Mesh Dependency

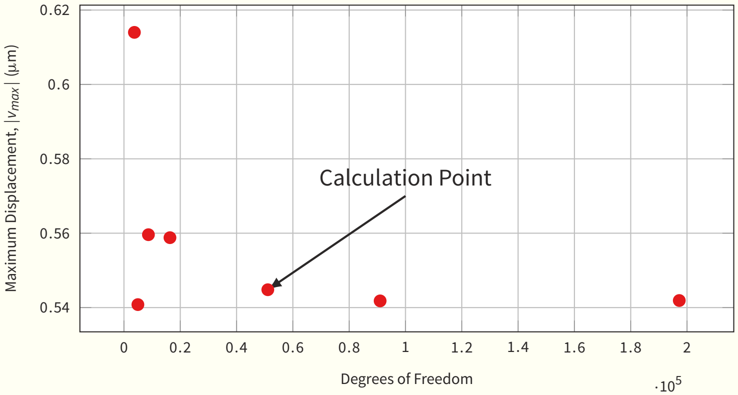

Additional Figures

- Additional Slides
- NPUAP Staging System
- Point Spread Function
- Quasi-Static Boundary Conditions
- Quasi-Static Error Comparison
- ARFI Boundary Conditions
- ARFI Error Comparison
- Shear Error Comparison

NPUAP Staging System

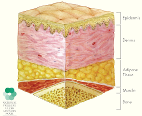

(a) Normal tissue

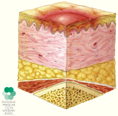

(b) Stage I

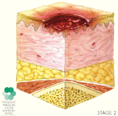

(c) Stage II

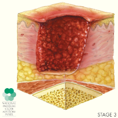

(d) Stage III

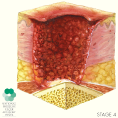

(e) Stage IV

(f) Unstageable

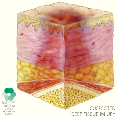

(g) Suspected DTI

Point Spread Function

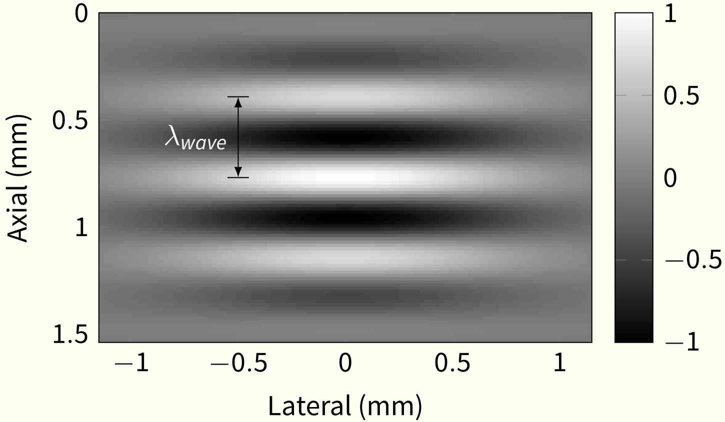

Point spread function used for simulating b-mode ultrasound scans. The function is defined axially by a cosine function at the probing frequency and modulated by a Gaussian function both axially and laterally.

QS USE Boundary Conditions

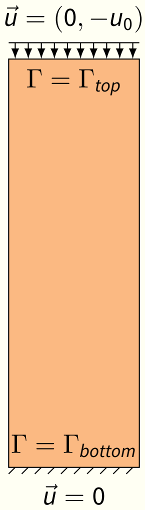

Boundary conditions used in the finite-element calculations of soft tissue deformation.

Quasi-Static Error

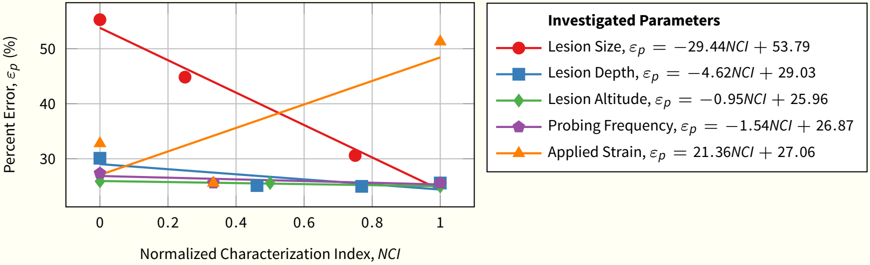

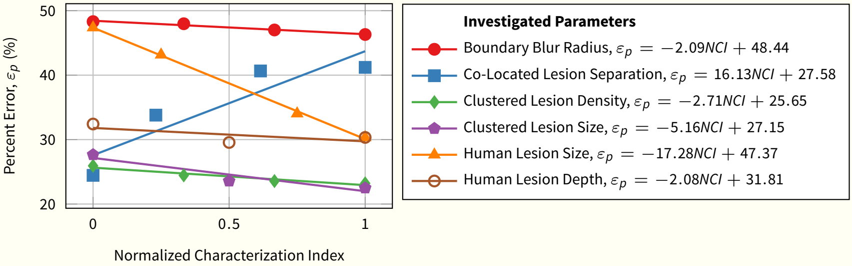

ARFI /Shear Boundary Conditions

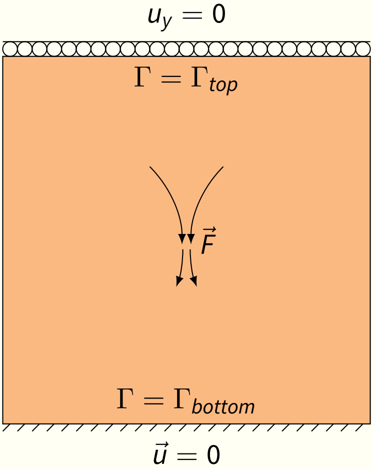

ARFI Error

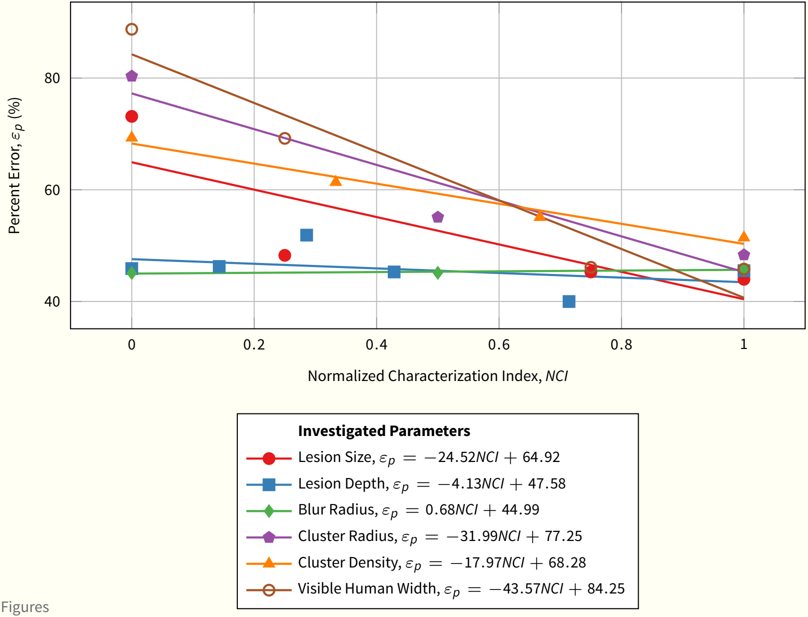

80
60
40
Percent Error, ε_p (%)
0
0.2
0.4
0.6
0.8
1
Normalized Characterization Index, *NCI*
Investigated Parameters
Lesion Size, $\varepsilon_p = -24.52NCI + 64.92$
Lesion Depth, $\varepsilon_p = -4.13NCI + 47.58$
Blur Radius, $\varepsilon_p = 0.68NCI + 44.99$
Cluster Radius, $\varepsilon_p = -31.99NCI + 77.25$
Cluster Density, $\varepsilon_p = -17.97NCI + 68.28$
Visible Human Width, $\varepsilon_p = -43.57NCI + 84.25$

Shear Error

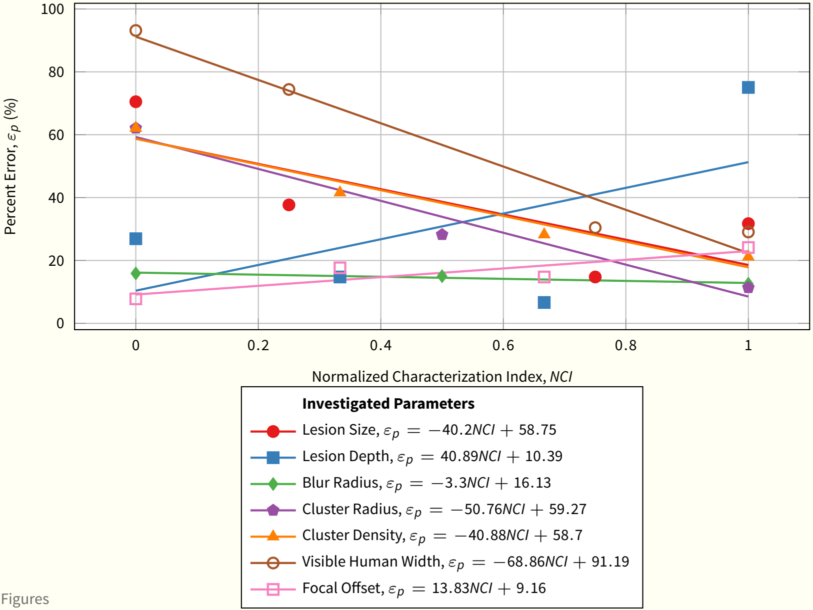

100
80
60
40
20
0
Percent Error, ε_p (%)
0
0.2
0.4
0.6
0.8
1
Normalized Characterization Index, *NCI*
Investigated Parameters
Lesion Size, $\varepsilon_p = -40.2NCI + 58.75$
Lesion Depth, $\varepsilon_p = 40.89NCI + 10.39$
Blur Radius, $\varepsilon_p = -3.3NCI + 16.13$
Cluster Radius, $\varepsilon_p = -50.76NCI + 59.27$
Cluster Density, $\varepsilon_p = -40.88NCI + 58.7$
Visible Human Width, $\varepsilon_p = -68.86NCI + 91.19$
Focal Offset, $\varepsilon_p = 13.83NCI + 9.16$